Temperature-insensitive Line Ratios

by

Anthony Kesich

Submitted to the MIT Department of Physics
in partial fulfillment of the requirements for the degree of

Bachelor of Science

at the

MASSACHUSETTS INSTITUTE OF TECHNOLOGY

June 2009

Author .....
MIT Department of Physics
May 21, 2009

Certified by .....
David P. Huenemoerder
Thesis Supervisor, Department of Physics
Thesis Supervisor

Accepted by .....
Professor David E. Pritchard
Senior Thesis Coordinator, Department of Physics

Abstract

We develop method to extract elemental abundance ratios using temperature-insensitive ratios of x-ray line fluxes for a collisionally ionized plasma. This method is then refined using more realistic plasma models for coronae of active stars. We finally apply the method to multiple sources and compare the results to those obtained via Emission Measure Modeling.

I. INTRODUCTION

Stellar evolution is governed by a handful of different quantities, such as density and rotation, just to name a few. One of the more important set of quantities is stellar elemental abundances. These abundances play a major role in determining the star's emission spectrum, but also play a more important, yet less well understood role in stellar evolution. The abundances derived from the spectrum only apply for the corona. However, these values can be used to derive internal abundances both in the case of isolated stars [1] and those with accretion disks [4, 8]. Therefore, it is important that we catalog elemental abundances in many stars in order to examine trends in stellar behavior.

Traditionally, abundances are calculated via spectral modeling. In this process, a synthetic spectrum is created from a set of given parameters. The synthesized spectrum is then folded through the instrumental parameters of the observing device and compared to the observed spectrum. If the two spectra are close enough to each other according to some fit criteria, then the process is over. Otherwise, the generating parameters are altered and the process is repeated. This process is summarized in Fig. 1.

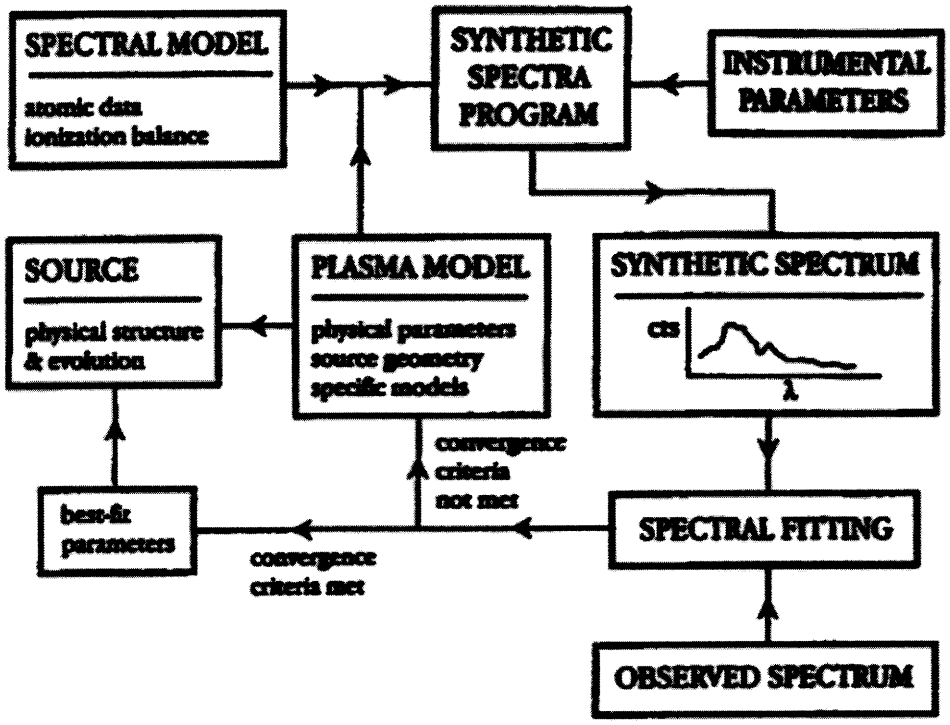

FIG. 1: Flow diagram of the spectral fitting process. Taken from Mewe 1999.

This process of fitting and refitting can often take many hours depending on the power of the machine and how many different variables you let "float" during the calculation. This method also requires us to constrain such things as temperature distributions, densities, and interstellar absorption coefficients. Due to the fundamental complexity of the atomic emissivities, the basic emission equations cannot be directly inverted. Also, since general solutions are non-unique, it is desirable to have an alternate method to compare against. If all we are truly looking for is the elemental abundances, this information can be superfluous.

In this paper, we will derive a system to calculate ratios of elemental abundances from observed X-ray spectra using a method independent of the plasma temperature distribution. This method will have the advantage of being much quicker than the standard spectral fitting since it will neglect quantities which are unneeded for abundance determination. We will then apply this method to several example spectra whose properties have already been calculated using the standard fitting method and compare the results. Finally, we will explore possible improvements and modifications that could be made to the method via further research.

II. BACKGROUND

The Chandra X-ray Observatory (CXO) is one of NASA's four Great Observatories. Launched in 1999, Chandra is currently one of the most sensitive X-ray telescope in operation. It can detect photons in the energy range of 80 eV to 8 keV (150 Å to 1.5 Å) and has a spectral resolving power of $\lambda/\Delta\lambda > 500$ [9]. The high resolution of Chandra's X-ray grating spectrometers allows the telescope to differentiate fine details in high-energy spectra previously unresolvable.

We can learn a lot about the structure of stellar objects through analysis of X-ray emissions. These high energy ($\geq$ 120 eV) photons are especially interesting due to the production processes behind them. Photons in this range are typically produced by one of two methods in stellar coronae.

The first of these is thermal Bremsstrahlung radiation. Significant continuum X-ray emissions occur in Chandra's observation range when temperatures are roughly between 1 million and 100 million Kelvin. By looking at the shape and size of the continuum spectrum, we can get a rough estimate on the temperature of the emitting star.

The second major type of emission is spectral lines generated by atomic transitions. Lines appear as sharp, discrete spikes in the emission spectrum. These lines are sensitive to both temperature and elemental abundances. By measuring these lines, we can reconstruct the plasma properties and the elemental abundances. However, as mentioned before, this can be a long and complicated process.

III. APPROACH

Our goal here is to find a combination of line fluxes that, when evaluated, is a function only of the ratio of the two elemental abundances. Specifically, it must be independent of temperature (to first-order).

A. Emissivities

The strength of individual lines are primarily a function of three variables: plasma temperature, elemental abundance, and emissivity. Emissivity is an atomic property of the element and is only dependent on temperature. The luminosity of the line is then: [3]

$$L_x = A_z \int \epsilon_x(T) D(T)\, \mathrm{dlog}\, T \text{ [ergs/sec]} \tag{1}$$

where A_z is the elemental abundance, $\epsilon_x(T)$ is the emissivity profile of the line in question in units of [photons cm^3/sec], and D(T) is the differential emission measure (DEM) defined as [6]:

$$D(T) = n_e(T) n_H(T) \frac{\mathrm{d}V}{\mathrm{d}\log T} \text{ [cm}^{-3}\text{]} \tag{2}$$

where $n_e(T)$ and $n_H(T)$ are the number density of electrons and Hydrogen, respectively, at a given temperature. The DEM can be viewed as a weighting function which tells us how much any range of temperatures contributes to the behavior and characteristics of the overall plasma.

The flux as viewed from a distance, d, is then:

$$F_x = \frac{A_z}{4\pi d^2} \int \epsilon_x(T) D(T)\, \mathrm{dlog}\, T \text{ [ergs/cm}^2\text{/sec]} \tag{3}$$

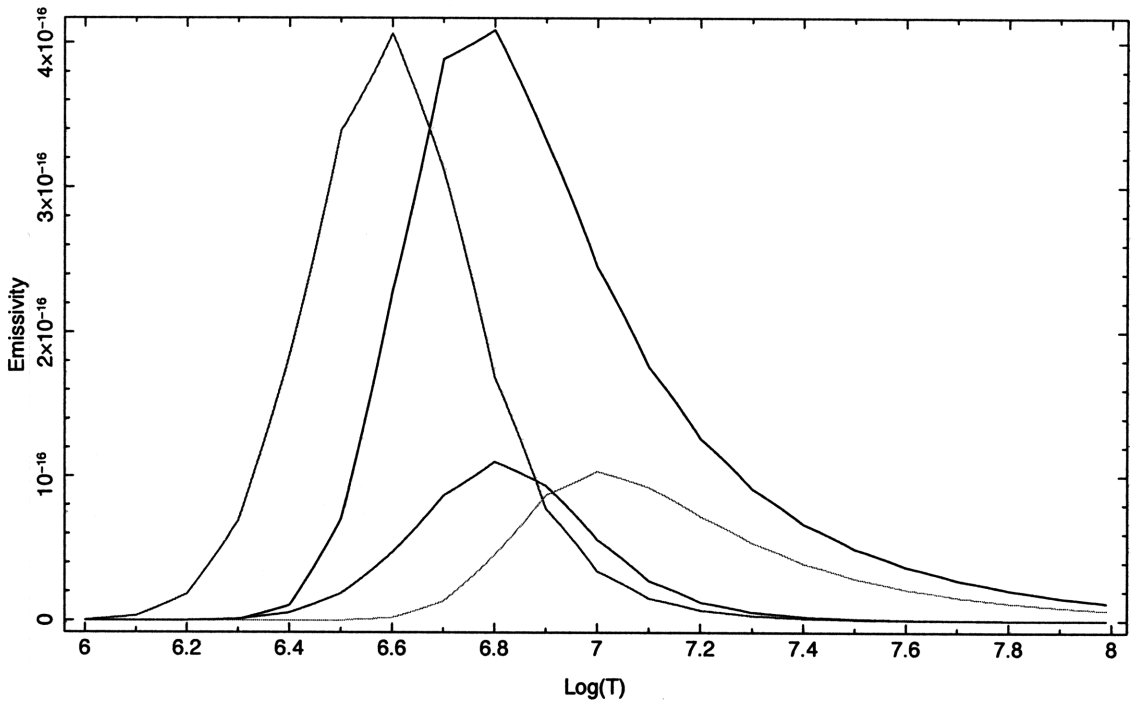

FIG. 2: Neon and Magnesium emissivities. Black: Ne X Lyman-α, Red: Ne IX He-like Resonance, Blue: Mg XII Lyman-α, Green: Mg XI He-like Resonance. Note how even though the amplitudes differ, the shapes are similar.

Emissivity is steeply peaked and far from constant with temperature. However, if we compare similar lines of different elements, such as Ne X Lyman-α to Mg XII Lyman-α, we notice that the shapes of the emission profiles are alike (see Fig. 2). Therefore, we should be able to take a linear combinations of lines of one element and create a profile similar to the other. By dividing, we can cancel out the dependence on temperature but retain information on abundances.

B. Ratios

To create a flat ratio, we divide fluxes in the following way:

$$r = \frac{F_{1,1} + aF_{1,2}}{bF_{2,1} + cF_{2,2}} = \frac{A_1}{A_2} \frac{\int (\epsilon_{1,1}(T) + a\epsilon_{1,2}(T)) D(T)\, \mathrm{dlog}\, T}{\int (b\epsilon_{2,1}(T) + c\epsilon_{2,2}(T)) D(T)\, \mathrm{dlog}\, T} \tag{4}$$

where $F_{x,y}$ refers to the observed flux of line y from element x.

We want to choose the three parameters, a, b, and c, such that the quotient on the right

is as close to 1 as possible. That is, we want to make the terms in parentheses in (4) as close to equal as possible. This requires a search over a three-dimensional parameter space. However, we can reduce it to a two parameter search by redefining the problem.

If we rewrite the ratio as such:

$$r = \frac{A_1}{A_2}\left(\frac{1}{b}\right)\frac{\int(\epsilon_{1,1}(T) + a\epsilon_{1,2}(T))D(T)\,\mathrm{dlog}\,T}{\int(\epsilon_{2,1}(T) + c'\epsilon_{2,2}(T))D(T)\,\mathrm{dlog}\,T} \tag{5}$$

where $c' \equiv c/b$, we just need to search for the a and c' which minimizes the variance of the quotient on the right. The parameter b can be later chosen to normalize the ratio and will depend on the lines used.

This is similar to the technique used by Liefke et. al. [5].

C. Finding Ratio Coefficients

Now that the problem has been reduced to a simple two-parameter space, finding we can find the optimal choices of a and c'. We can simply do an exhaustive search over a reasonable grid of parameters. Setting A_1, A_2, and b to 1 for now, we can define a fit statistic to minimize over.

One such choice of statistic is:

$$stat = \left(\frac{var(r)}{avg(r)}\right)^2 \tag{6}$$

This choice is useful in that it minimized the inherent fluctuation in the model.

We also usually restrict our search to line ratios involving elements where $\Delta Z \leq 2$. As seen in Fig. 2, this lets us keep the peaks of the emissivities near each other which allows us to make a flatter ratio. The lines used for each element and the corresponding wavelengths are summarized in Table I.

The results of five ratio minimizations are summarized in Table II. The ratio involving Sulfur and Oxygen is also included even though it violates our rule of $\Delta Z \leq 2$. We make this exception since Sulfur and Oxygen tend to be strong lines, so even though there is a lot of noise in the method, you can still make a rough determination. As an example, the ratio of Silicon to Sulfur using the coefficients from the table is show in Fig. 3 against Log(T). The part of the temperature range where the emissivities are negligible is ignored.

Element	Line	λ (Å)
Ne	Ne X HLa	12.13
	Ne IX HeLar	13.45
Mg	Mg XII HLa	8.42
	Mg XI HeLar	9.17
Si	Si XIV HLa	6.18
	Si XIII HeLar	6.65
S	S XVI HLa	4.73
	S XV HeLar	5.04
O	O VII HLa	18.97
	O VI HeLar	21.60

TABLE I: Lines used in calculating the ratios and their corresponding wavelengths.

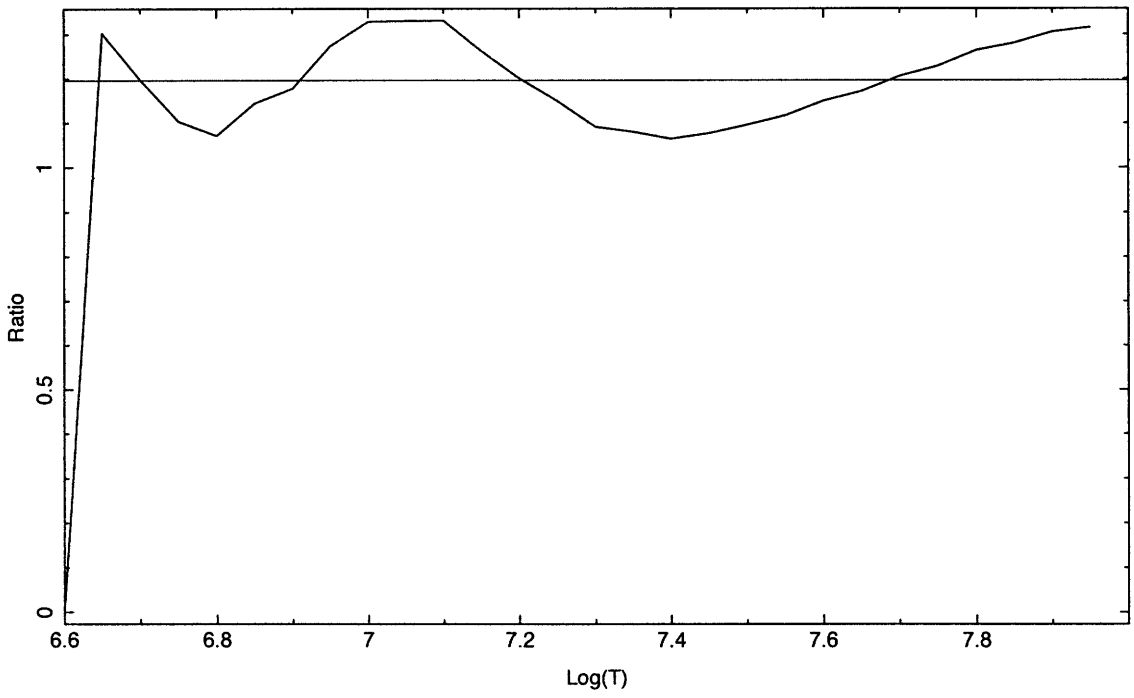

FIG. 3: The line ratio for Silicon to Sulfur plotted against log(T). The red line shows the average value of the ratio.

Ratio	a	c'	Mean	Std
Ne to Mg	0.05	2.675	1.440	0.273
Mg to Si	0.085	1.920	0.536	0.064
Si to S	0.125	1.545	1.197	0.092
S to O	2.99	0.00	0.212	0.137
Ne to O	2.59	0.00	0.347	0.120

TABLE II: Coefficients and corresponding ratio statistics. The Mean and Std columns refer to the average value and standard deviation of the ratio over temperature for where the emissivities, and therefore the resultant line fluxes, are non-negligible. Note that these statistics are calculated for abundance normalized to the sun (i.e. A_z=1 means the abundance of z is equal to the solar abundance of z.

Using the results calculated, we can now define our b. As said above, b is a normalization coefficient such that the ratios come out to be 1 if the abundances are equal. Therefore, we can just define b to be the mean of the calculated ratios. We can even go one step further and include the deviation from constant in the value b. This allows us to keep track of the different systematic errors associated with the different ratios. For example, $b_{\mathrm{Ne/Mg}} = 1.44 \pm 0.273$.

Now we have all the data to build our relationship:

$$\frac{A_1}{A_2} = \left(\frac{1}{b}\right) \frac{F_{1,HLa} + aF_{1,HeLar}}{F_{2,HLa} + c'F_{2,HeLar}} \tag{7}$$

The HLa subscript stands for Hydrogen-like Lyman-α line and HeLar stands for the Helium-like Lyman-α resonance line. This equation is valid for all stellar emissions assuming that the line emissions are non-negligable.

IV. EXAMPLES AND COMPARISON

It this section, we apply the temperature-insensitive method to a few example stars. We then compare these results to those derived via emission measure modeling. Finally, we look at how changes over time in ratios can give insightful information.

HR 5110 Characteristics	
Spectral Type	K0 IV
Mass	0.8 $M_\odot$
Radius	3.4 $R_\odot$
Orbital Period	2.6 days
Inclination	8.9°
Distance	44.5 pc
L_x(0.5-7.0 keV) [10^{30} ergs/sec]	4.6

TABLE III: Properties of the star HR 5110 [2]

A. HR5110

HR 5110 is a binary system with one active component. It is emissive in the X-ray spectrum and the system is nearly pole-on, so HR 5110 is never eclipsed by the companion star. This makes it an ideal candidate for exploration with Chandra. Its properties are summarized in Table III.

The X-ray spectrum, shown in Fig. 4, was collected by Chandra in two sessions, one of 38.5 ks and one of 39.5 ks, for a total of almost 22 hours of observation.

To determine the line fluxes, we first build a continuum model of the spectrum by ignoring regions containing lines. We then use this model as a baseline against which to measure the actual line fluxes. This was accomplished by fitting a 3-temperature plasma model to the spectrum with the lines removed. Once we had this baseline value, we fit Gaussian functions to the lines with floating. The models have floating areas and floating but bounded centers. The width of the line is fixed by the resolving power of Chandra. Fits were done in small wavelength intervals containing prominent features. Often multiple gaussians were used in a single fit to constrain blended lines and other small features. An example of a fit to Ne X Lyman-α is shown in Fig. 5. Values for the lines we will use in temperature-insensitive ratios are summarized in Table IV.

After fitting to all of the prominent lines in the spectrum, we used the observed fluxes to reconstruct the DEM. This process also generated values for elemental abundances. Elemental abundance ratios made using these values are documented in Table IV A and compared

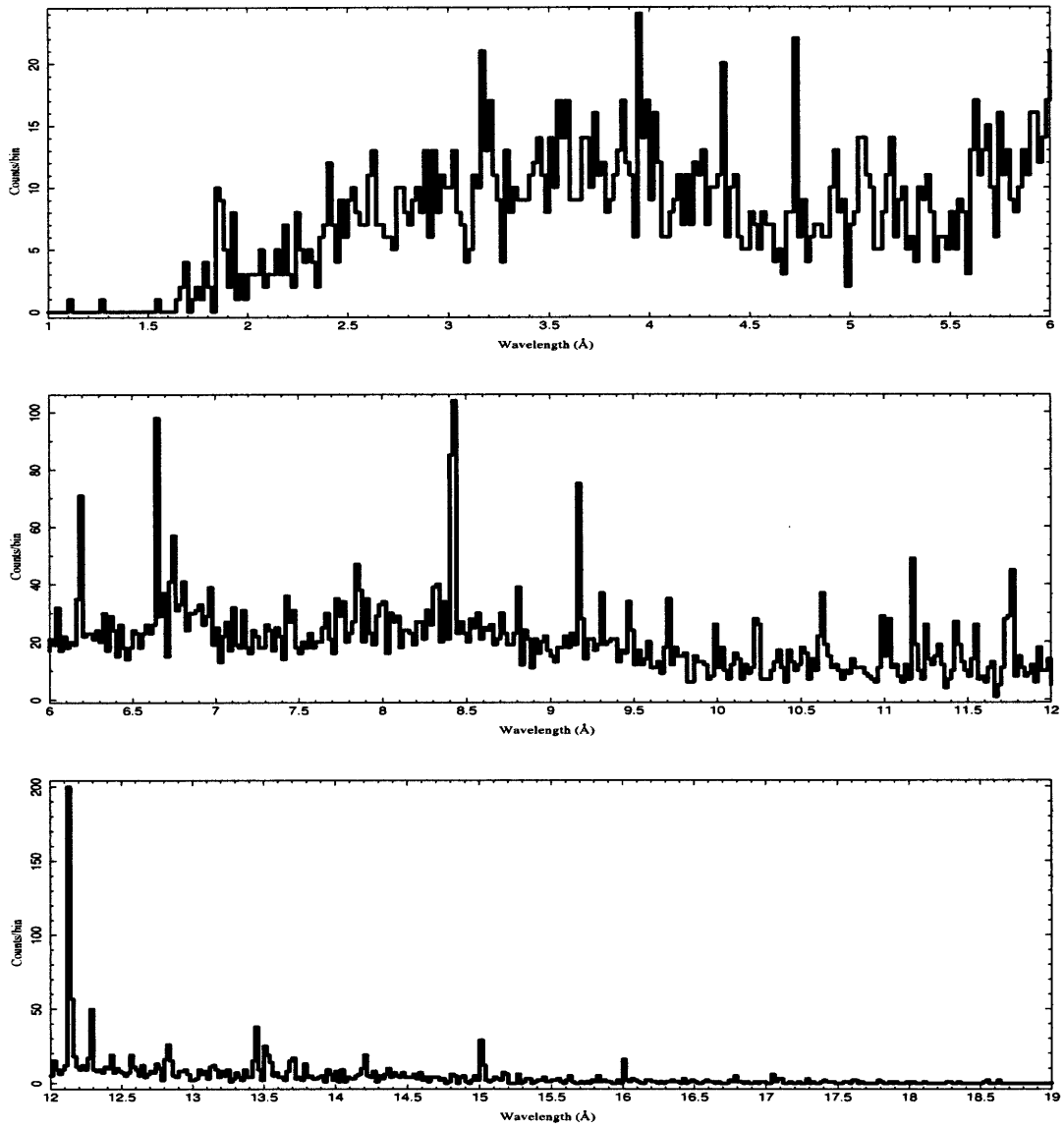

FIG. 4: HR 5110 Spectrum as observed by the High Energy Grating on Chandra.

to the results found using eq. (7). When comparing the two methods, all of the ratios fall within 2σ of each other.

Over the period of observation, Chandra recorded 3 different flares in HR 5110 where the X-ray count rate increased by a factor of 1.5-2 (See fig. 6). We therefore broke the spectrum up into flaring and quiescent sections. Performing spectral fitting for these sections gave us new line values also shown in Table IV A. Note that even though the value for the OVII Lyman-α resonance line is missing due to its faintness in the recorded spectrum, we can still do the calculations. As Table IV shows, the coefficient multiplying its flux is zero. The

Line	Full	Flaring	Quiescent
NeX Lα	31.7±0.63	29.8±1.34	23.1±0.97
NeIX Lαr	9.22±0.58	8.35±1.87	5.04±0.97
MgXII Lα	5.11±0.14	5.83±0.32	4.41±0.27
MgXI Lαr	2.92±0.16	3.50±0.38	1.91±0.22
SiXIV Lα	2.21±0.10	2.77±0.31	1.51±0.16
SiXIII Lαr	2.78±0.12	3.13±0.27	1.68±0.18
SXVI Lα	1.23±0.17	7.12±0.61	0.53±0.17
SXV Lαr	2.55±0.43	3.13±0.54	0.48±0.18
OVIII Lα	44.0±1.96	48.0±4.37	36.2±3.10
OVII Lαr	4.94±1.09	undetected	5.86±2.08

TABLE IV: Measured fluxes for HR 5110. Fluxes are in units of [10^{-5}photons/cm^2/s].

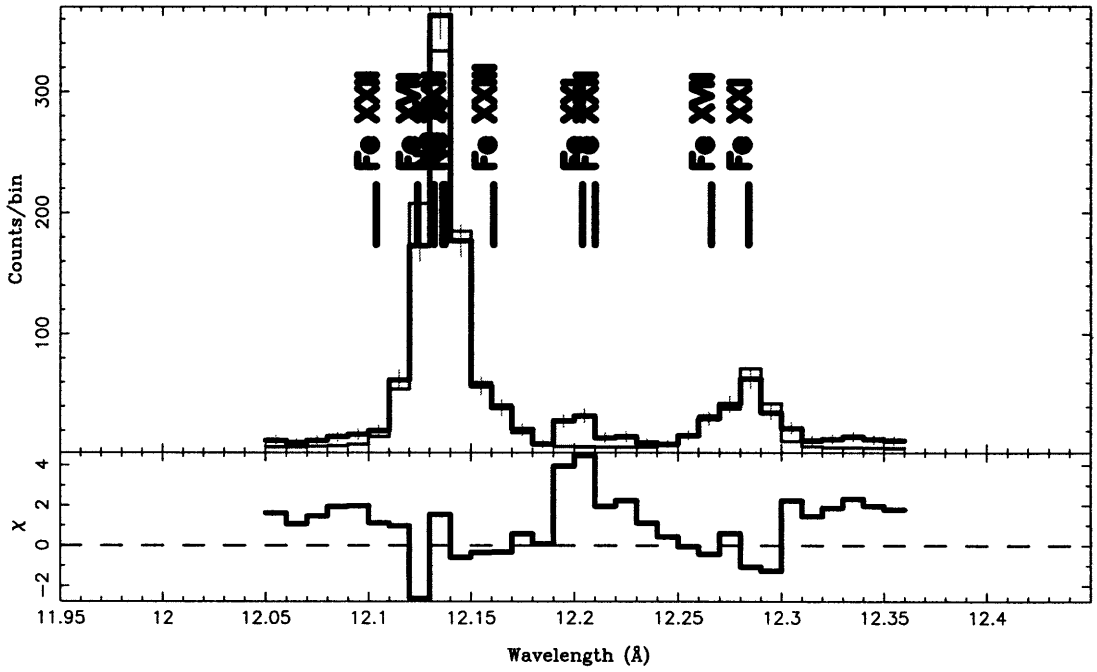

FIG. 5: Example of a fit to NeX Lyman-α (12.13 Å) and surrounding lines (12.16 Å, 12.17 Å, 12.19 Å). The black line is the observed spectrum. The other is the model. Residuals are plotted along the bottom.

Ratio	DEM value	T-insens value
Ne to Mg	2.31±0.11	1.73±0.33
Mg to Si	1.65±0.15	1.32±0.17
Si to S	0.60±0.15	0.41±0.07
S to O	1.34±0.36	0.95±0.63

TABLE V: Ratios of elemental abundances derived from a DEM fit and from temperature-insensitive ratios for HR5110. The uncertainty given is 1σ.

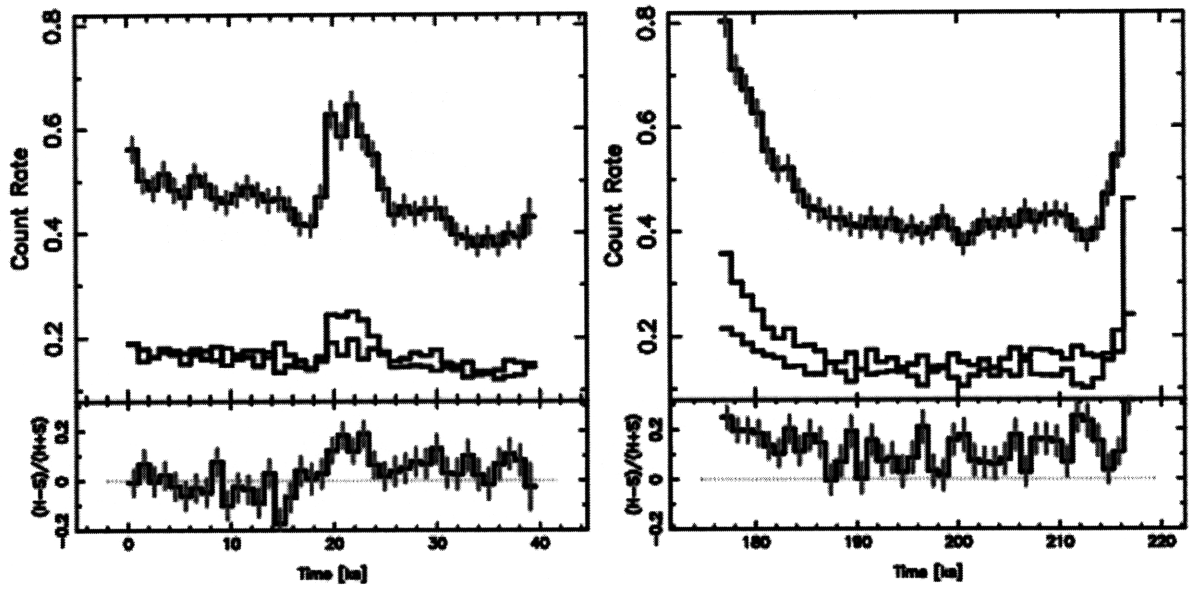

FIG. 6: HR5110 light curve for both observations by Chandra. The black curve is for the full X-ray band (1.7-25 Å), the blue curve is the hard band (1.7-8.0 Å), and the red curve is the soft band (11-25 Å).

ratios calculated for these two cases are summarized in Table VI.

The interesting thing to note is the behavior of the Si/S ratio and the S/O ratio. During active flares of the star, the Si/S ratio drops and the S/O ratio rises. This leads us to the possible conclusion that the relative abundance of S in the corona increases during flares. This seems more likely than the chance that both silicon and Oxygen both drop. The intersting thing to note here is that we were able to come to this conclusion by only measuring a handful of line fluxes and calculating a few algebraic expressions. If we wanted to measure this via traditional emission measure reconstruction, it would require the fitting

Ratio	Flaring	Quiescent
Ne to Mg	1.38±0.29	1.71±0.35
Mg to Si	1.30±0.19	1.81±0.28
Si to S	0.22±0.03	1.12±0.32
S to O	1.62±1.07	0.26±0.18

TABLE VI: Temperature insensitive abundance ratios calculated for flaring and quiescent periods of HR 5110.

	HR 1099		θ^1 Ori E		AB Dor [7]		TW Hydrae	
Ratio	DEM	T-insens	DEM	T-insens	DEM	T-insens	DEM[8]	T-insens[4]
Ne to Mg	-	3.01±0.57	2.2±0.2	1.67±0.34	3.29±1.16	1.82±0.36	-	-
Mg to Si	-	0.92±0.11	1.1±0.1	1.00±0.14	1.21±0.41	0.62±0.08	-	-
Si to S	-	0.97±0.09	1.4±0.4	1.25±0.16	0.54±0.23	0.62±0.09	-	-
S to O	-	0.38±0.24	1.9±0.8	1.43±0.97	0.89±0.40	1.38±0.91	-	-
Ne to O	-	-	7.11±3.0	4.88±2.76	-	-	9.77±1.9	5.8±2.2

TABLE VII: Abundance ratios calculated vie DEM reconstruction against temperature-insenssitive qualities for three different stars.

of over 100 lines total and hours of processing time.

B. Other Stars

HR 1099, θ^1 Ori E, and AB Dor are three stars observed by Chandra with well exposed spectra of the line fluxes. The fluxes for HR 1099 and θ^1 Ori E were computed the same way as outlined for HR 5110. The abundances were derived via the same DEM reconstruction methods. The ratios are summarized in Table VII.

The two methods correlate well for θ^1 Ori E. The results for each of the four calculated ratios are within 1σ of each other.

V. CONCLUSION

Using temperature-insensitive line ratios to measure abundance ratios gives us another tool for measuring stellar properties. Since DEM reconstruction is non-unique, it also gives us another reference point to check against. If all we are concerned with is measuring relative abundances, this method is much quicker than reconstructing the DEM, so more data can be processed in a short period of time. Finally, comparing ratios from different activity levels of a star can lead to insights on how abundances behave with coronal activity.

Acknowledgments

DPH is awesome. So are NSS and Paula.

---

[1] J. J. Drake and P. Testa. The 'solar model problem' solved by the abundance of neon in nearby stars. *Nature*, 436:525–528, July 2005.

[2] D. P. Huenemoerder, R. A. Osten, A. Kesich, P. Testa, and N. Schulz. Polar Exploration and Coronal Structure in the Active Binary HR 5110. In E. Stempels, editor, *American Institute of Physics Conference Series*, volume 1094 of *American Institute of Physics Conference Series*, pages 656–659, February 2009.

[3] David P. Huenemoerder, Claude R. Canizares, , and Norbert S. Schulz. X-Ray Spectroscopy of II Pegasi: Coronal Temperature Structure, Abundances, and Variability. *The Astrophysical Journal*, 559(2):1135–1146, 2001.

[4] J. H. Kastner, D. P. Huenemoerder, N. S. Schulz, C. R. Canizares, and D. A. Weintraub. Evidence for Accretion: High-Resolution X-Ray Spectroscopy of the Classical T Tauri Star TW Hydrae. *The Astrophysical Journal*, 567:434–440, March 2002.

[5] C. Liefke, J. . Ness, J. H. M. M. Schmitt, and A. Maggio. Coronal properties of the EQ Peg binary system. *Astronomy and Astrophysics*, 000:(in press), October 2008.

[6] Rolf Mewe. *X-ray Spectroscopy in Astrophysics.* Springer, New York, NY, 1999.

[7] J. Sanz-Forcada, A. Maggio, and G. Micela. Three years in the coronal life of AB Dor. I. Plasma emission measure distributions and abundances at different activity levels. *ASTRON.ASTROPHYS.*, 408:1087, 2003.

[8] B. Stelzer and J. H. M. M. Schmitt. X-ray emission from a metal depleted accretion shock onto the classical T Tauri star TW Hya. *Astronomy and Astrophysics*, 418:687–697, May 2004.

[9] M. C. Weisskopf, B. Brinkman, C. Canizares, G. Garmire, S. Murray, and L. P. Van Speybroeck. An Overview of the Performance and Scientific Results from the Chandra X-Ray Observatory. *The Publications of the Astronomical Society of the Pacific*, 114:1–24, January 2002.